Volume 12
Number 21
7 June 2021
Pages 3069-3212

Polymer Chemistry

rsc.li/polymers

ISSN 1759-9962

ROYAL SOCIETY OF CHEMISTRY

COMMUNICATION

Sandra Schlögl *et al.*

Locally controlling dynamic exchange reactions in 3D printed thiol-acrylate vitrimers using dual-wavelength digital light processing

Polymer Chemistry

ROYAL SOCIETY OF CHEMISTRY

COMMUNICATION

View Article Online
View Journal | View Issue

Cite this: *Polym. Chem.*, 2021, **12**, 3077

Received 27th March 2021,
Accepted 5th May 2021

DOI: 10.1039/d1py00427a

rsc.li/polymers

Locally controlling dynamic exchange reactions in 3D printed thiol-acrylate vitrimers using dual-wavelength digital light processing†

Elisabeth Rossegger, Khadijeh Moazzen, Mathias Fleisch and Sandra Schlögl *

Vitrimers are covalent adaptable polymer networks, which are able to rearrange their topology in response to an external stimulus. Below the topological freezing temperature (T_v) they behave like a classic thermoset, whilst above T_v, they become malleable, weldable and recyclable. However, vitrimers mainly rely on thermo-activated dynamic exchange reactions, which suffer from a lack in spatial control. Herein, we introduce triphenylsulfonium phosphate as a latent transesterification catalyst, which releases strong Brønsted acids upon UV exposure (365 nm). Once locally formed, the acids are able to efficiently catalyse thermo-activated transesterifications as confirmed by stress relaxation studies. The latent catalyst is introduced into visible light (405 nm) curable thiol-acrylate resins, whose fast curing kinetics enable the additive manufacturing of precise 3D objects. Due to the orthogonality between the curing reaction and the photo-activation of the catalyst, transesterifications can be selectively switched on in the photo-cured vitrimer simply by UV-light exposure. By using a dual-wavelength digital light processing 3D printer, operating at 405 and 365 nm, the catalyst is locally activated during the layer-by-layer build-up of the 3D structures. This enables the fabrication of soft active devices, which undergo locally controlled topology arrangements above the networks' T_v.

Covalent adaptable networks (CANs) contain dynamic bonds which break and reform either autonomously or upon an external stimulus. The bond exchange is based on interactions between repeating units, following either an associative (bond forming/breaking mechanism) or a dissociative (bond breaking/forming mechanism) pathway.[1] In associative bond exchange mechanisms, intermediate reactants are formed, which increase the crosslink density temporarily. However, as soon as the new crosslink is formed, the former bond is cleaved, which leads to a nearly constant crosslink density.[2]

In thermo-activated systems, the topological freezing transition temperature (T_v) is crucial as it governs the kinetics of the exchange reactions and thus, influences the flow behavior of the associative CANs. Above T_v, the exchange reactions become macroscopically relevant and a material flow is observed following an Arrhenius trend, comparable to silica-based glasses. Thus, the dynamic networks behave like reshapeable, malleable and re-processable fluids.[3] Below T_v, the exchange reactions are slow and the network properties are comparable to a permanently crosslinked thermoset.[1,2,4,5] It should be noted that the T_v is influenced by numerous parameters involving crosslink density, exchange reaction kinetics (based on catalyst loading, favored chemical affinity between reactants and thermodynamic factors), monomer mobility or stiffness of the network.[4]

Leibler and co-workers coined associative CANs, whose viscosity follows the Arrhenius law above the T_v, vitrimers.[6] They prepared epoxy-acid and epoxy-anhydride networks, which were able to undergo thermo-activated transesterifications.[7] Based on the kinetics of the bond exchange reactions, the networks could be reprocessed, welded, reshaped and healed at temperatures well above the T_v.[8] Due to the high number of commercially available monomers and easy implementation in numerous application fields, vitrimers based on transesterification chemistry are still one of the most prominent classes of associative CANs reported in literature.[5,9] However, these dynamic networks require an appropriate transesterification catalyst, which accelerates the bond exchange reactions. Commonly used catalysts for transesterifications are Brønsted acids, organo-metallic complexes and organic bases.[10]

Current research is geared towards the processing of vitrimers with additive manufacturing techniques to obtain personalized 3D structures with improved functionality. In particular, Shi *et al.* developed thermosetting epoxy inks for direct ink writing at elevated temperatures. By dissolving the printed objects in ethylene glycol at elevated temperatures, the ink was recycled and used for further printing processes.[11]

Bowman *et al.* reported a recyclable thiol–ene photopolymer for photolithographic applications, which was able to undergo

Polymer Competence Center Leoben GmbH, Roseggerstrasse 12, A-8700 Leoben, Austria. E-mail: sandra.schloegl@pccl.at

†Electronic supplementary information (ESI) available: FTIR spectra, DSC and TGA curves of the thiol-acrylate vitrimer. See DOI: 10.1039/d1py00427a

thiol–thioester exchange reactions.[12] Zhang and co-workers developed a photo-curable resin formulation with hydroxyl-functional mono- and diacrylates, a Norrish Type I photo-initiator and $Zn(OAc)_2$ for catalyzing the transesterification reactions, which endowed the network with thermal mendability and reprocessability.[13] Inspired by this work, we recently expanded this concept towards 3D printable thiol-acrylate vitrimers by introducing organic phosphates as alternative transesterification catalysts.[14] Due to the excellent solubility and catalytic efficiency of the new catalyst, we were further able to design acrylate-based vitrimers for high resolution 3D printing.[15] The thereby used additive manufacturing method of DLP (digital light processing) 3D printing is already a well-established technology and enables the fabrication of complex structures with good resolution.[16]

Whilst these concepts enable a localized solidification of the material by photo-induced curing processes, the subsequent thermo-activation of the exchange reactions lacks from a spatial control. In previous work, a local control of the exchange reactions was realized by introducing nano-sized fillers with photothermal properties into epoxy-acid and epoxy-anhydride vitrimers.[17] The fillers efficiently convert light to heat and by employing NIR lasers as light source, localized healing, welding and shape memory was demonstrated.[18] Furthermore, Bowman *et al.* demonstrated the spatiotemporal photo-triggered formation of a basic and an acidic catalyst, which promote or halt dynamic exchange reactions in thin photocurable films at room temperature.[19]

Herein, we follow a completely new approach to manufacture 3D objects that undergo spatially controlled topological rearrangements. By exploiting orthogonal photoreactions, a thiol-acrylate system is cured by long-wavelength irradiation (405 nm) (Fig. 1c), whilst the transesterification catalyst is activated upon short-wavelength irradiation (365 nm) (Fig. 1d). With dual-wavelength digital light processing (DLP) 3D printing, operating at 405 and 365 nm, the catalyst is activated locally during the layer-by-layer build-up of the 3D structures (Fig. 1b). Multi-wavelength printing *via* vat photopolymerization has already been used to control photoinitiation and -inhibition simultaneously in volumetric polymerization[20] and to selectively adjust the material performance in multi-material approaches.[21]

For the network design, a photocurable thiol-acrylate formulation (resin-ER-1) is applied, whose vitrimeric properties and 3D processability have been demonstrated in a recent work.[14] The resin contains mono- and bi-functional acrylate monomers bearing functional –OH groups, which promote exchange reactions in the cured photopolymer network.[22] In addition, 25 mol% of a tri-functional thiol crosslinker and 2 wt% phenylbis(2,4,6-trimethylbenzoyl)phosphine oxide as long-wavelength absorbing photoinitiator are added to the formulation. However, the transesterification catalyst is replaced with an onium salt acting as latent transesterification catalyst (resin-ER-1-lat) (Fig. 1a). Using a photoacid generator (PAG) as transesterification catalyst enables a spatiotemporal control of exchange reactions and temperature as well as UV-light are required as external triggers to activate the exchange reactions in the dynamic network (Fig. 1e).

Onium salts have been introduced by Crivello in the late 1970s and are widely used to initiate cationic polymerization and curing of epoxides.[23] Upon UV exposure, onium salts undergo a cleavage reaction and, by subsequent reaction with solvents or monomers of the formulation, form strong Brønsted acids.[24]

The acidic strength of the released acid depends on the nucleophilicity of the counter-anion, with stronger acids being generated with lower nucleophilic counter-anions.[24,25] They are easily soluble in numerous monomers and provide a temperature stability up to 180 °C.[26] To ensure the orthogonality between the curing reaction and the activation of the catalyst,

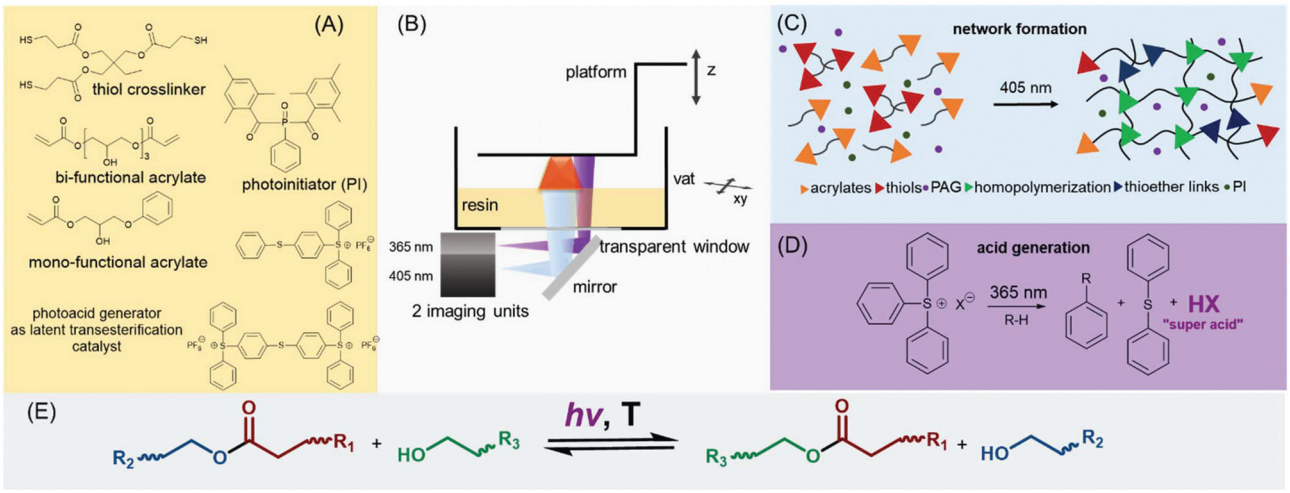

Fig. 1 (a) Monomers and latent transesterification catalyst used for the preparation of the 3D printable thiol-acrylate vitrimer. (b) Schematic representation of the dual-wavelength DLP process. (c) Visible light curing of thiol-acrylate monomers and UV triggered activation of Brønsted acids acting as transesterification catalyst. (e) Transesterification process after photoacid generation *via* UV-light at elevated temperatures.

the triphenylsulfonium phosphate was used as latent catalyst, which is transparent at 405 nm. In contrast to diaryliodonium salts, triphenylsulfonium salts have a low reduction potential and do not promote radical induced cationic polymerizations.[27] Consequently, the photolytically formed radicals from the curing reaction cannot be oxidized by triphenylsulfonium phosphate.

As shown in FT-IR experiments, following the time-dependent depletion of the characteristic absorption bands of acrylate and thiol groups at 1635 and 2570 cm^{-1}, the cure kinetics is not affected by the addition of 10 wt% triphenylsulfonium phosphate (Fig. S1 and S2, ESI†). The maximum conversion of thiol and acrylate groups (50% and 100% respectively) is obtained upon 60 s of light exposure at 405 nm.

Due to its fast cure speed, sufficiently low viscosity (894 mPa s) and shelf life of at least 72 h, resin-ER-1-lat can be applied in 3D printing techniques relying on vat polymerization. In particular, digital light processing (DLP) was chosen, in which the 3D object is built-up *via* a layer-by-layer solidification of the photo-reactive resin formulation.

For rheological experiments, discs with a diameter of 10 mm were printed with a wavelength of 405 nm and the stress relaxation of the network (between 140 and 180 °C) was determined prior to and after UV exposure at 365 nm (Fig. 2a). Under the applied conditions, the network is stable as confirmed by thermogravimetric analysis (Fig. S3, ESI†). In addition, the applied temperatures in the stress relaxation studies were well above the glass transition of the network, which amounted to 10.8 °C (DSC curve is shown in Fig. S4, ESI†).

After curing, resin-ER-1-lat exhibited a slight stress relaxation, which is comparable to a resin formulation containing no triphenylsulfonium phosphate (resin-ER-1-ref). Thus, the results suggest that the slight decrease in stress relaxation is not related to a premature release of acids (either photochemically induced or by thermal decomposition of the triphenylsulfonium salt) but can be attributed to a thermal release of volumetric shrinkage stresses arising during network evolution.[28]

Upon subsequent UV exposure, a rapid stress relaxation was observed for resin-ER-1-lat, with 63% of the initial stress being relaxed within 53.5 min. The results clearly show that the photochemically released Brønsted acids are able to efficiently catalyze thermo-activated transesterifications. It is well known that Brønsted acids are able to catalyse esterifications as well as transesterifications.[29] The reaction mechanism involves the protonation of the oxygen of the carbonyl ester group, which increases the electrophilicity of the adjoining carbon atom.[30] The protonated carbonyl group is more reactive towards a nucleophilic attack and it readily forms a tetrahedral intermediate with an available –OH group in the network. This is followed by a proton transfer and the departure of the leaving group. A new ester bond is formed whilst the acidic catalyst (H^+) is regenerated.

The acid-catalysed transesterification is temperature-dependent, which is also in agreement with the stress-relaxation experiments. By increasing the temperature from 140 to 180 °C, a faster decrease of the stress relaxation is observed giving rise to a higher bond exchange rate at increasing temperature.

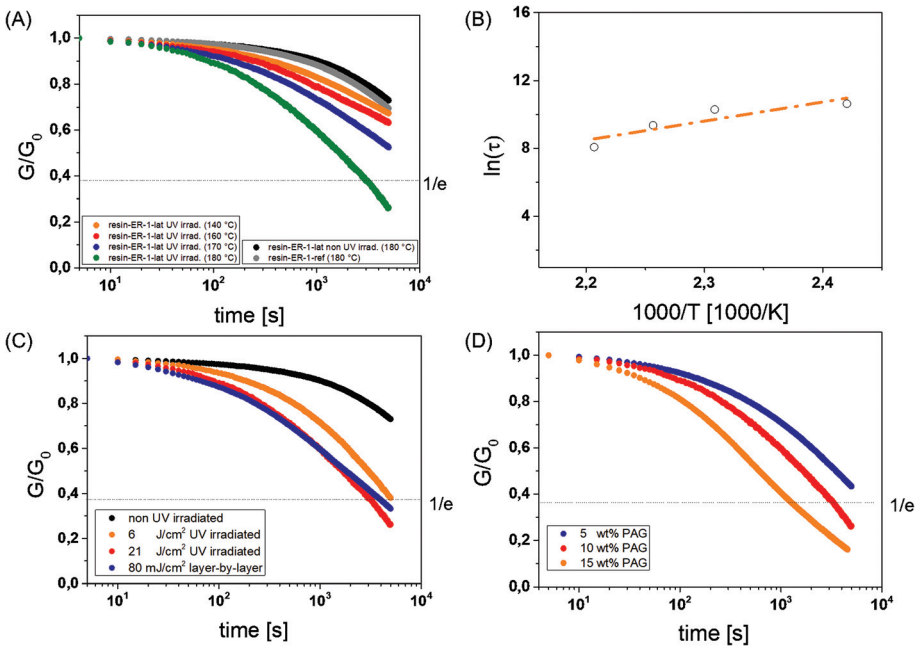

Fig. 2 (a) Normalised stress relaxation curves of UV activated resin-ER-1-lat *versus* temperature in comparison to the non UV irradiated resin-ER-1-lat and the reference (resin-ER-1-ref) containing no triphenylsulfonium phosphate. (b) Arrhenius plot of UV activated resin-ER-1-lat derived from measured relaxation times. Normalised stress relaxation curves of UV activated resin-ER-1-lat obtained at 180 °C as a function of time, depending on (c) the exposure dose and (d) the catalyst content.

Besides temperature, the exchange rate is also increasing with higher catalyst concentration.[31] In terms of triphenylsulfonium phosphate acting as photolatent catalyst, the number of released Brønsted acids can be increased either by extending the exposure time or by increasing the salt concentration in the formulation. Fig. 2c shows the stress relaxation (at 180 °C) of UV activated resin-ER-1-lat as a function of the exposure dose, whilst keeping the catalyst content constant (10 wt%). A clear acceleration of the stress relaxation kinetics is observed at higher exposure dose, confirming a faster bond exchange rate due to the release of a higher number of Brønsted acids.

The same trend is observed, albeit at a higher extend, when increasing the amount of triphenylsulfonium phosphate from 5 to 15 wt% (Fig. 2d). The results evidence that both catalyst content and exposure dose influence the stress relaxation kinetics of vitrimers containing triphenylsulfonium phosphate as photolatent catalyst.

By using the Maxwell Model, the characteristic relaxation times (τ^*) were taken as the time required to relax to $1/e$ of the initial stress at temperatures between 140 and 180 °C.[31] Fig. 2b clearly shows that the stress relaxation data of UV activated resin-ER-1-lat satisfies the Arrhenius law and confirms the vitrimeric nature of the irradiated resin-ER-1-lat. The activation energy (E_a) was estimated from the slope ($m = E_a/R$) of the straight line fitted to the data, and amounted to 93.7 kJ mol^{-1}.

To demonstrate the network's ability to locally switch on the exchange reactions on demand, 3D objects were manufactured with dual-wavelength DLP 3D printing, operating at two different wavelengths (405 and 365 nm). During the printing process, resin-ER-1-lat is selectively crosslinked layer-by-layer upon visible light irradiation (405 nm) without activation of the catalyst. The set-up allows for an additional spatially controlled exposure at 365 nm of the desired layers which enables curing and photoacid generation at the same time. Thus, the catalyst is selectively activated layer-by-layer and in a controlled lateral manner.

Test structures were printed, in which selected areas were UV exposed layer-by-layer during the printing process as shown in Fig. 3a and b to induce the curing of the network and the activation of the photoacid simultaneously. To confirm the localized activation of topological rearrangements in the 3D objects, selected reshaping experiments were carried out (Fig. 3c and d).

In the first step, a rectangular shaped test specimen (shape I in Fig. 3c) was placed in a U-shaped mold and heated at 120 °C for 240 min. One half of the test specimen was UV exposed at 365 nm during the printing and thus, contained the activated transesterification catalyst (Fig. 3a). At 120 °C, the network is able to undergo topological rearrangements in the UV-irradiated part of the test specimen. A remolding of the exposed half of the samples takes place as the network changes from an elastic solid to a viscoelastic liquid, which has been shown in the stress relaxation curves (Fig. 2a). The test specimen was then cooled to room temperature (rt) and removed from the mold. The freestanding sample was able to retain its U-shaped form at 10 °C (shape II in Fig. 3c).

By heating the sample well above its T_g to 100 °C for 10 min, the non-exposed half was able to move back to its original flat position, whilst the exposed half was locked and maintained its angle (shape III in Fig. 3c). In the non-exposed area, the photopolymer network recovers its original shape since the

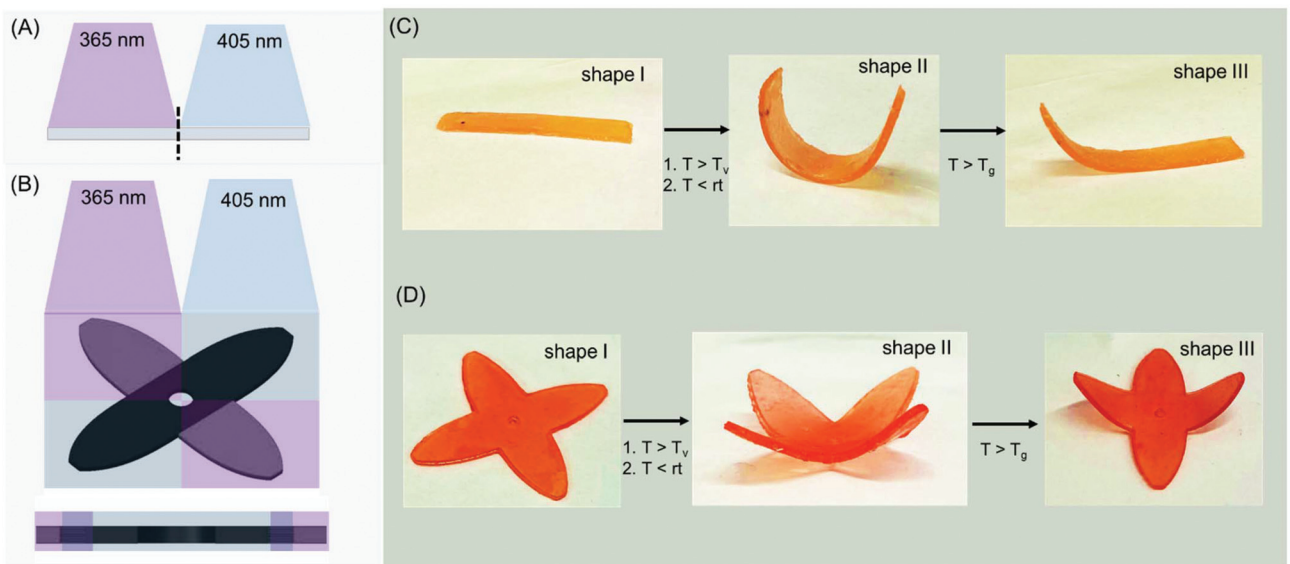

Fig. 3 Illustrations monitoring the (a and b) printing set-up of the rectangular test structures and the grippers, and the programming and locally controlled reshaping of (c) rectangular test structures and (d) grippers obtained from resin-ER-1-lat. The test structures were fabricated by dual-wavelength DLP 3D-printing operating at 405 nm and 365 nm. During the layer-by-layer exposure at 405 nm the resin was solidified and selective areas of the test structures were exposed at 365 nm to cure and release Brønsted acids acting as transesterification catalyst simultaneously.

elongated polymer chains return to their entropically more favorable initial state above the network's T_g to release the stresses induced by the shape change.

In contrast, in the exposed area, transesterification reactions occurred due to the photo-released Brønsted acids and caused a rearrangement of the network to the U-shaped mold. The induced stresses were released by dynamic exchange reactions within the UV-activated regions while keeping the crosslink density constant. Consequently, rising the temperature above the network's T_g did not lead to a shape recovery of the UV-exposed part.

As additive manufacturing techniques benefit from a high freedom in design, the concept can be easily transferred to other 3D structures. In another experiment, a gripper was 3D printed, whose arms were selectively exposed at 365 nm (shape I in Fig. 3d). After the programming step, a selective movement of the non-exposed arms is realized, whilst the exposed arms remain locked in their programmed positions due to the acid-catalyzed topological rearrangements (shape III in Fig. 3d).

The results evidence that the use of triphenylsulfonium phosphate as photolatent transesterification catalyst enables a spatially resolved activation of topological rearrangements in vitrimers. By transferring the concept to 3D printable resin formulations, functional 3D structures are obtained, whose vitrimeric properties can be precisely controlled layer-by-layer by using a dual-wavelength DLP 3D printer.

Conclusions

Summing up, a photolatent catalyst was employed for the local activation of topological rearrangements in thermo-activated vitrimers. Triphenylsulfonium phosphate was chosen as photolatent catalyst, as it benefits from a high temperature stability, is transparent in the visible light region and releases strong Brønsted acids upon UV exposure. By using the photolatent catalyst in a visible light curable thiol-acrylate vitrimer, selective curing of the photopolymer network at 405 nm was achieved without premature release of Brønsted acids. Subsequent UV exposure at 365 nm triggered the formation of Brønsted acids, which efficiently catalyzed transesterifications. Stress relaxation studies confirmed the vitrimeric properties of the photo-activated networks and revealed that the relaxation kinetics increase with rising temperature, exposure doses as well as catalyst content.

The photoreactive nature of the resin enabled the transfer of the concept towards 3D structures, which were fabricated with a dual-wavelength DLP printer, operating at 405 and 365 nm. Selective movement of the 3D structures was accomplished after a programming step above the network's T_v, due the localized activation of the catalyst during the printing process. Thus, the use of photolatent catalysts in photo-reactive vitrimer systems is a versatile strategy to fabricate soft active devices, which are able to undergo locally programmable shape change.

Experimental section

Materials

Trimethylolpropane tri(3-mercaptopropionate) was obtained from Bruno Bock (Germany) and all other chemicals were purchased from Sigma-Aldrich and used as received.

Preparation of resin-ER-1-lat

Sudan II (0.01 wt%), 2-hydroxy-2-phenoxypropyl acrylate (50 mol%) and glycerol 1,3-diclycerolate diacrylate (25 mol%) were mixed with 5–15 wt% triarylsulfonium hexafluorophosphate solution in an ultrasonic bath until the photoabsorber was dissolved. 2 wt% phenylbis(2,4,6-trimethylbenzoyl) phosphine oxide and 25 mol% trimethylolpropane tri(3-mercaptopropionate) were added and dissolved by stirring the formulation at 45 °C. Sudan II is used as a photoabsorber to increase the resolution during the printing process. To avoid a too high absorption by the dye, which could hinder the activation of the photoacid, only 0.01 wt% were used.

Characterization

Light-induced curing of resin-ER-1 was followed by FTIR spectroscopy utilizing a Vertex 70 spectrometer (Bruker, USA). 16 scans were accumulated in transmission mode from 4000 to 700 cm^{-1} with a resolution of 4 cm^{-1} and the absorption peak areas were determined with OPUS software. 1 μL of the resin was drop-cast between two CaF_2 discs and cured with a light emitting diode lamp (zgood® wireless LED curing lamp) comprising a power density of 3.5 mW cm^{-2} (λ = 420–450 nm). Thermal gravimetrical analysis was carried out with a Mettler Toledo (USA) TGA/DSC thermogravimetric analyzer. The measurements were performed under nitrogen atmosphere by heating the sample from 23 to 900 °C with a heating rate of 10 °C min^{-1}.

Differential scanning calorimetry measurements were carried out with a PerkinElmer DSC 4000 instrument (USA). A temperature program from −30 to 100 °C with a heating rate of 10 K min^{-1} was applied under nitrogen atmosphere. The T_g was determined from the second heating run by taking the midpoint in heat capacity.

The viscosity of the resin was characterized by using a modular compact rheometer MCR 102 from Anton Paar (Austria) with a CP60-0.5/TI cone (49.97 mm diameter and 1.982° opening angle). The measurements were conducted with a shear rate ramp from 0.1 to 300 s^{-1} at 25 °C.

Stress relaxation experiments at temperatures between 140 and 180 °C were performed on a moving die rheometer from Anton Paar (Austria). The samples were balanced to the selected measurement temperature for 20 min. Subsequently, a 1% step strain was inserted and the decreasing stress was recorded over time.

DLP 3D printing

A dual-wavelength DLP 3D-printer prototype (with 405 and 365 nm light sources) from Way2Production (Austria) was used for 3D printing experiments (Fig. S5†). To cure the network

without activating the photolatent catalyst, one bottom layer was exposed for 10 s (to obtain a good adhesion to the building platform), whereas the other layers were illuminated for 7 s (related to the double bond conversion obtained from FT-IR kinetic studies) with the 405 nm light source. The activation of the photoacid generator and the simultaneous curing of the network was achieved by irradiating the desired layers upon 10 s (compromise between sufficient activation and resolution) exposure with UV-A light (365 nm). The layer height was set to 50 μm. All the printed specimen were post-cured for 10 min upon 405 nm light exposure and thermally treated for 2 h at 120 °C.

Re-shaping experiments

Re-shaping experiments were carried out with 3D printed grippers (d = 35 mm) and a 3D printed rectangular test specimen (l = 40 mm, b = 5 mm, h = 1 mm), which were heated to 140 °C for 4 h, to fix the first shape. The second shape was programmed by heating the sample to 120 °C for 4 h in a mold. For fixing the second shape, the sample was cooled down to 0 °C. By heating up to 100 °C, the first shape was regained in the non-exposed areas.

Conflicts of interest

There are no conflicts to declare.

Acknowledgements

Part of the research work was performed within the COMET-Module "Chemitecture" (project-no.: 21647048) at the Polymer Competence Center Leoben GmbH (PCCL, Austria) within the framework of the COMET-program of the Federal Ministry for Transport, Innovation and Technology and the Federal Ministry for Digital and Economic Affairs with contributions by Montanuniversitaet Leoben (Institute of Chemistry of Polymeric Materials). The PCCL is funded by the Austrian Government and the State Governments of Styria, Upper and Lower Austria.

In addition, part of the research work was also performed with the "SMART" project. This project has received funding from the European Union's Horizon 2020 research and innovation programme under the Marie Sklodowska-Curie grant agreement no. 860108.

References

1 W. Zou, J. Dong, Y. Luo, Q. Zhao and T. Xie, *Adv. Mater.*, 2017, **29**, 1606100.
2 J. M. Winne, L. Leibler and F. E. Du Prez, *Polym. Chem.*, 2019, **10**, 6091–6108.
3 L. Tuan, B. Zhao and J. Zhang, *Polymer*, 2020, **194**, 122392.
4 W. Denissen, J. M. Winne and F. E. Du Prez, *Chem. Sci.*, 2016, **7**, 30–38.
5 M. Guerre, C. Taplan, J. M. Winne and F. E. Du Prez, *Chem. Sci.*, 2020, **11**, 4855–4870.
6 D. Montarnal, M. Capelot, F. Tournilhac and L. Leibler, *Science*, 2011, **334**, 965–968.
7 N. J. Van Zee and R. Nicolaÿ, *Prog. Polym. Sci.*, 2020, **104**, 101233.
8 (*a*) S. Kaiser, J. N. Jandl, P. Novak and S. Schlögl, *Soft Matter*, 2020, **16**, 8577–8590; (*b*) S. Kaiser, S. Wurzer, G. Pilz, W. Kern and S. Schlögl, *Soft Matter*, 2019, **15**, 6062–6072; (*c*) M. Giebler, C. Sperling, S. Kaiser, I. Duretek and S. Schlögl, *Polymers*, 2020, **12**, 1148.
9 M. Capelot, D. Montarnal, F. Tournilhac and L. Leibler, *J. Am. Chem. Soc.*, 2012, **134**, 7664–7667.
10 W. Alabiso and S. Schlögl, *Polymers*, 2020, **12**, 1660.
11 Q. Shi, K. Yu, X. Kuang, X. Mu, C. K. Dunn, M. L. Dunn, T. Wang and H. Jerry Qi, *Mater. Horiz.*, 2017, **4**, 598–607.
12 C. Wang, T. M. Goldman, B. T. Worrell, M. K. McBride, M. D. Alim and C. N. Bowman, *Mater. Horiz.*, 2018, **5**, 1042–1046.
13 B. Zhang, K. Kowsari, A. Serjouei, M. L. Dunn and Q. Ge, *Nat. Commun.*, 2018, **9**, 1831.
14 E. Rossegger, R. Höller, D. Reisinger, J. Strasser, M. Fleisch, T. Griesser and S. Schlögl, *Polym. Chem.*, 2021, **117**, 10212.
15 E. Rossegger, R. Höller, D. Reisinger, M. Fleisch, J. Strasser, V. Wieser, T. Griesser and S. Schlögl, *Polymer*, 2021, **221**, 123631.
16 M. Pagac, J. Hajnys, Q.-P. Ma, L. Jancar, J. Jansa, P. Stefek and J. Mesicek, *Polymers*, 2021, **13**(4), 598.
17 (*a*) Y. Yang, Z. Pei, X. Zhang, L. Tao, Y. Wei and Y. Ji, *Chem. Sci.*, 2014, **5**, 3486–3492; (*b*) Z. Wang, Z. Li, Y. Wei and Y. Ji, *Polymers*, 2018, **10**, 65.
18 Z. Feng, J. Hu, H. Zuo, N. Ning, L. Zhang, B. Yu and M. Tian, *ACS Appl. Mater. Interfaces*, 2018, **11**, 1469–1479.
19 B. T. Worrell, M. K. McBride, G. B. Lyon, L. M. Cox, C. Wang, S. Mavila, C.-H. Lim, H. M. Coley, C. B. Musgrave, Y. Ding and C. N. Bowman, *Nat. Commun.*, 2018, **9**, 2804.
20 M. P. de Beer, H. L. van der Laan, M. A. Cole, R. J. Whelan, M. A. Burns and T. F. Scott, *Sci. Adv.*, 2019, **5**, eaau8723.
21 J. J. Schwartz and A. J. Boydston, *Nat. Commun.*, 2019, **10**, 791.
22 M. Hayashi and R. Yano, *Macromolecules*, 2019, **53**, 182–189.
23 (*a*) J. V. Crivello, *Adv. Polym. Sci.*, 1984, **62**, 3–48; (*b*) J. V. Crivello, *J. Polym. Sci., Part A: Polym. Chem.*, 1999, **37**, 4241–4254.
24 J. V. Crivello and J. H. W. Lam, *J. Polym. Sci., Polym. Chem. Ed.*, 1979, **17**, 977–999.
25 M. Sangermano, I. Roppolo and A. Chiappone, *Polymers*, 2018, **10**, 1–8.
26 T. J. Spencer and P. A. Kohl, *Polym. Degrad. Stab.*, 2011, **96**, 686–702.
27 Y. Yağci and I. Reetz, *Prog. Polym. Sci.*, 1998, **23**, 1485–1538.
28 J. Chen, S. Jiang, Y. Gao and F. Sun, *J. Mater. Sci.*, 2018, **53**, 16169–16181.

29 A. Streitwieser, C. H. Heathcock and E. M. Kosower, *Introduction to organic chemistry*, 4th edn, 1998.
30 (*a*) E. Lotero, Y. Liu, D. E. Lopez, K. Suwannakarn, D. A. Bruce and J. G. Goodwin, *Ind. Eng. Chem. Res.*, 2005, **44**, 5353–5363; (*b*) P. A. Alaba, Y. M. Sani and W. M. A. W. Daud, *RSC Adv.*, 2016, **6**, 78351–78368.
31 M. Capelot, M. M. Unterlass, F. Tournilhac and L. Leibler, *ACS Macro Lett.*, 2012, **1**, 789–792.